

# Transient-Pulse Behavior and Self-Induced Transparency\*

FREDERIC A. HOPF†

*Air Force Cambridge Research Laboratories, Bedford, Massachusetts 07130*  
and

*Massachusetts Institute of Technology, Cambridge, Massachusetts 02139*

AND

MARLAN O. SCULLY‡

*Department of Physics and Materials Science Center, Massachusetts Institute of Technology, Cambridge, Massachusetts 02139*

(Received 19 February 1969)

The dynamics of self-induced transparency in an inhomogeneously broadened attenuator is investigated with special emphasis on delay times. One finds a strong dependence of delay times on the input value of the area parameter  $\theta$  with pulses of  $\theta_{in} \approx \pi$  exhibiting much larger delay times than for  $\theta_{in} = 2\pi$ . This investigation is extended to include the effects of an atomic phase memory time  $T_2$  which is of the order of ten times the pulse width (i.e., in accord with current experimental circumstances). The variation of other parameters is considered. A method of measuring  $\theta$  directly is presented.

THE problem of coherent pulse propagation through an inhomogeneously broadened medium has been the object of recent interest. As McCall and Hahn<sup>1</sup> have shown, when a pulse is produced with appropriate area  $\theta = (\varphi/\hbar) \int dt \mathcal{E}(t, z) = 2\pi$ , where  $\varphi$  is the dipole-matrix element  $ex_{ab}$  and configuration (hyperbolic secant), it may pass through an attenuating medium unchanged with a delay time of  $t_D \approx \frac{1}{2}\alpha L \hat{t}$ . Here  $\alpha$  is the attenuation coefficient,  $\hat{t}$  is the pulse width, and the Beer's Law attenuation for a rod of length  $L$  is  $e^{-\alpha L}$ . The self-induced-transparency effect has been investigated experimentally<sup>1,2</sup> and delay times of the right order of magnitude were reported.

In as much as the quantity  $\theta$  is the direct interest, a simple means of measuring it is presented in this communication. Furthermore, we wish to investigate the dynamical evolution of a pulse as it develops into a hyperbolic-secant shape. This is accomplished by numerically integrating the equations which couple the electromagnetic pulse and the atomic system.<sup>3</sup> This allows for considerable flexibility, since one may then include in the investigation the roles of the atomic phase memory time  $T_2$ , the atomic lifetime  $T_1$ , scattering loss, detuning, etc., as they affect the evolution of the pulse. The results of this analysis are at variance with the experimental results of Ref. 2.

The theoretical development is a self-consistent treatment which involves coupling Maxwell's and Schrödinger's equations.<sup>4</sup> An electromagnetic wave of

\* Paper based in part on a thesis submitted by F. A. Hopf to Yale University in partial fulfillment of the requirements for the Ph.D. degree.

† Paper written while the author was pursuing an NRC-OAR. Postdoctoral Resident Research Associateship.

‡ Work supported in part by the Advanced Research Projects Agency Contract No. 50-90, and in part by the National Aeronautics and Space Administration.

<sup>1</sup> S. L. McCall and E. L. Hahn, Phys. Rev. Letters **18**, 908 (1967).

<sup>2</sup> C. K. N. Patel and R. E. Slusher, Phys. Rev. Letters **19**, 1019 (1967).

<sup>3</sup> F. A. Hopf and M. O. Scully, Phys. Rev. **179**, 399 (1969).

<sup>4</sup> W. E. Lamb, Jr., Phys. Rev. **134**, A1429 (1964); C. K. Rhodes, A. Szoke, and A. Javan, Phys. Rev. Letters **16**, 1151 (1968); private communication; and to be published.

the form

$$E(t, z) = \mathcal{E}(t, z) \cos(kz - vt) \quad (1)$$

interacting with an inhomogeneously broadened ensemble of two-level atoms [with a frequency distribution  $\sigma(\omega)$ ] leads to the equations

$$\begin{aligned} \partial \mathcal{E}(t, z) / \partial z + (1/c) \partial \mathcal{E}(t, z) / \partial t \\ = -\alpha \int_{-\infty}^t dt' \mathcal{E}(t', z) \exp[-(t-t')/T_2] \\ \times \chi(t-t', t', z) - \kappa \mathcal{E}(t, z), \quad (2) \\ \partial \chi(T, t, z) / \partial t \end{aligned}$$

$$\begin{aligned} = -\varphi^2 / 2\hbar^2 \int_{-\infty}^t dt' \mathcal{E}(t, z) \mathcal{E}(t', z) \exp[-(t-t')/T_2] \\ \times [\chi(T+t-t', t', z) + \chi(T-t+t', t', z)]. \quad (3) \end{aligned}$$

The velocity  $c$  is taken to be the velocity of light in the inert background and  $\kappa$  is the linear (unsaturable) loss per unit length due to scattering. The attenuation constant<sup>5</sup> is given by

$$\alpha = \varphi^2 N \pi \nu \sigma(\nu) / 2\hbar \epsilon, \quad (4)$$

where  $N$  is the number of atoms in the lower level minus the number in the upper level,  $\epsilon$  is the dielectric constant of the inert background, and the nonlinear susceptibility  $\chi(T, t, z)$  is the Fourier transform of the population density

$$\chi(T, t, z) = \int d\omega \sigma(\omega) [\rho_{bb}(\omega, t, z) - \rho_{aa}(\omega, t, z)] \cos \omega T. \quad (5)$$

When  $T_2 \gg \hat{t}$  and  $\kappa = 0$ , the quantity  $\theta$  obeys the equation

$$d\theta/dz = -(\frac{1}{2}\alpha) \sin \theta. \quad (6)$$

<sup>5</sup> In as much as this communication deals with an attenuator, it is convenient to choose  $\alpha$  as a positive number (i.e., an attenuation constant); as a consequence there is a possible confusion of sign between this work and that of Ref. 3 (i.e., here  $N$  goes as  $\rho_{bb} - \rho_{aa}$ , and likewise  $\chi$  differs from the notation of Ref. 3 by an over-all minus sign).

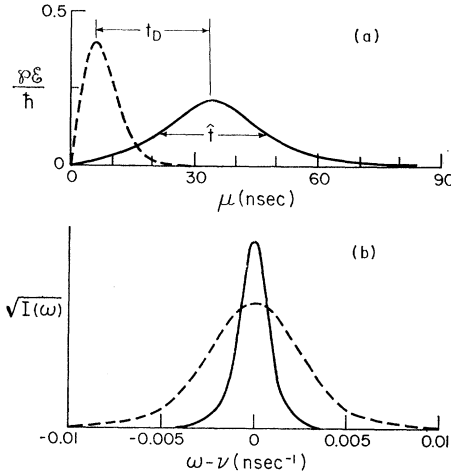


FIG. 1. In this figure, we show the results of a numerical calculation for an input pulse of 10 nsec in width and area  $1.3\pi$ . The medium is chosen so that  $T_1 \gg \hat{t}$ ,  $\kappa=0$ , and  $e^{-\alpha L}=0.0012$ . (a) We show the pulse envelopes  $\varphi \mathcal{E}(\mu, z)/\hbar$ , where  $\mu=t-z/c$ . The input pulse (broken curve) is at  $z=0$ ,  $\mu=t$ , and the output pulse (solid curve) is at  $z=L$ ,  $\mu=t-L/c$ . The leading edge of the pulse occurs at the left, and time flows to the right. The delay time  $t_D$  is as shown in the figure. The delay due to the inert background (relative to vacuum) is eliminated by choosing " $c$ " to the velocity of light in the background. (b) We show the square root of the power spectrum  $I(\omega, z)$  at  $z=0$  (input pulse, broken curve) and  $z=L$  (output pulse, solid curve). Note that  $[I(\nu, 0)]^{1/2} = 1.3\pi = \theta_{in}$  and  $[I(\nu, L)]^{1/2} = 1.9\pi = \theta_{out}$ .

The area is seen to converge on  $2n\pi$ , so that a pulse with  $\theta_{in}$  between  $\pi$  and  $3\pi$  will go to  $2\pi$  and one with  $\theta_{in}$  less than  $\pi$  will go to a  $\theta=0$  pulse. The energy of the pulse is proportional to the quantity  $\tau(z)$  where

$$\tau(z) = (\varphi/\hbar)^2 \int dt \mathcal{E}^2(t, z). \quad (7)$$

The pulse width  $\hat{t}$  is taken to be the full width at half-height of the envelope  $\mathcal{E}(t, z)$  and the delay time  $t_D(z)$  is the shift in the peak of the pulse relative to the velocity of light in the inert background (see Fig. 1). Equations (2) and (3) are solved numerically in order to obtain the quantities  $\theta$ ,  $\tau$ ,  $\hat{t}$ , and  $t_D$ .

In as much as the area  $\theta$  is of direct interest here we discuss its measurement. One way to measure  $\theta$  would be to shine the pulse on an atomic beam. The atoms at resonance with the carrier frequency would respond directly to  $\theta$  and by noting the extent to which the atomic wave function is changed,  $\theta$  could be inferred. This would not be easy and would fix  $\theta$  only up to a multiple of a constant angle. An easier and more direct method involves measuring the power spectral density, as measured by a spectrometer. In particular, if one writes

$$I(\omega, z) = (\varphi/\hbar)^2 \left| \int_{-\infty}^{\infty} dt \mathcal{E}(t, z) e^{-i(\omega-\nu)t} \right|^2, \quad (8)$$

then it is clear that

$$[I(\nu, z)]^{1/2} = \theta(z). \quad (9)$$

The quantity  $I(\omega, z)$  is proportional to the spectral density, and  $\theta^2$  will be proportional to the value of  $I$  at  $\omega=\nu$  as in Fig. 1(b).

We now turn to a discussion of the time evolution of the electromagnetic pulse. As is well known,<sup>1</sup> when a  $2\pi$  hyperbolic-secant pulse passes through an attenuating medium it will be delayed in time relative to where it would be if it were passing through the inert background. This time delay is a direct consequence of atomic coherence. We now wish to consider the delay times for an arbitrary ( $\theta \neq 2\pi$ ) situation. We will be particularly interested in the dependence of the delay times and pulse attenuation as a function of the energy of the input pulse, and we consider the change in these relationships as we vary  $T_1$ ,  $T_2$ , linear loss, and detuning from the center line. We will see that there are some particularly marked effects on the delay times as one varies the input-pulse amplitude. The delay times for  $\theta_{in} \approx \pi$  are shown to be proportional to  $\hat{t}_{in} \exp(\frac{1}{2}\alpha L)$  and these might differ by as much as several orders of magnitude from the delay time of the  $2\pi$  pulse (which goes linearly as  $\hat{t}_{in}\alpha L$ ). In each of the numerical integrations, the initial pulse shape is of the form  $\mathcal{E}(t, 0) = C_1 \exp(-t^2/C_2)$ , where  $C_1$  is adjustable, to give the proper value of  $\theta_{in}$ , and  $C_2$  is chosen to give an initial width of 10 nsec. The medium is chosen such that

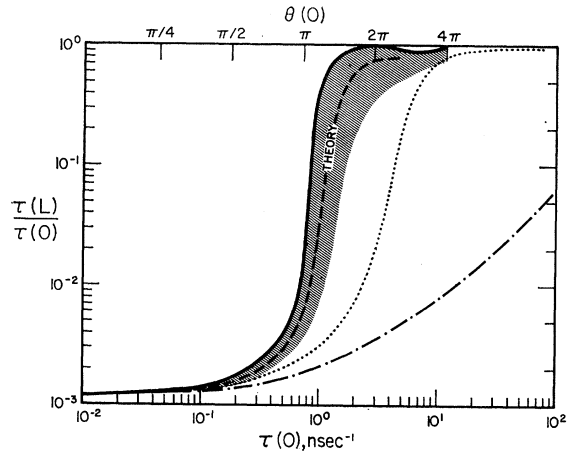


FIG. 2. This figure summarizes the results of the computer calculations for  $\tau_{out}/\tau_{in}$  versus  $\tau_{in}$ . The value of  $\theta_{in}$  corresponding to  $\tau_{in}$  is shown on the top scale. The solid curve is for the case  $T_2 \gg \hat{t}$ ,  $T_1 \gg \hat{t}$ ,  $\kappa=0$ , with no detuning. The dash curve gives the case  $T_2=50$  nsec. All of the other curves that we have obtained lie within the shaded region on the graph (the boundary represents the case of six degenerate sublevels). These results are to be contrasted with the dot-dash curve calculated from the data given in Fig. 1 of Ref. 2 (at a  $SF_6$  pressure of 0.021 T). The dotted curve is a saturation curve given in the limit that  $T_2 \ll \hat{t}$ . The formula used is given in Ref. 3. One notes that, on a log-log scale, there is not much difference between the steepness of the saturation and transparency curves.

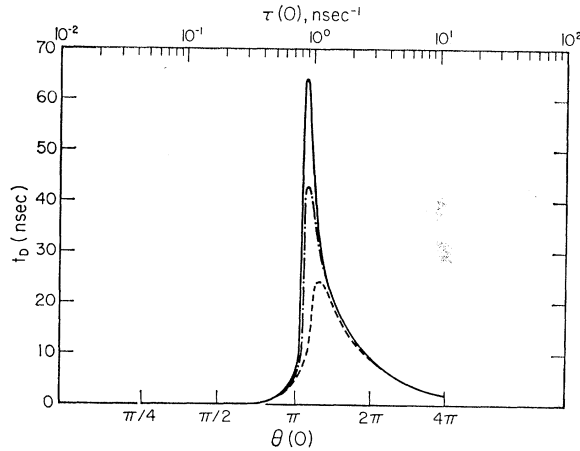


FIG. 3. In this figure, we show a plot of delay times versus input  $\theta$ . The delay time is illustrated in Fig. 1(a). The value of  $\tau_{in}$  corresponding to  $\theta_{in}$  is shown at the top scale. The solid curve is for the case  $T_2 \gg \hat{t}$ ,  $T_1 \gg \hat{t}$ ,  $\kappa = 0$ , with no detuning. The dot-dash curve is for the case  $T_2 = 150$  nsec and the broken curve is for the case  $T_2 = 50$  nsec. The other parameters are the same as with the solid curve.

$e^{\alpha L} = 0.0012$  and  $T_2^* = 1$  nsec. We vary the input  $\theta$  and the phase-memory time  $T_2$ . In Fig. 2, we show the attenuation of the pulse  $\tau_{out}/\tau_{in}$  as a function of  $\tau_{in}$  plotted on log-log paper (for the case of  $T_2 \gg \hat{t}$ ). In this figure, the transparency of the  $2n\pi$  pulse is evident, with the curve approaching unity for inputs of  $2\pi$  and  $4\pi$ . We note that there are significant deviations from the small-signal attenuation for input pulses as small as  $\frac{1}{2}\pi$ . The corresponding delay times are shown in Fig. 3. One notes that the delay times for  $\theta_{in} \approx \pi$  are very much larger than for  $\theta_{in} \approx 2\pi$ . This phenomenon can be understood by a fairly simple argument. For any fixed rod length  $L$ , one can choose a pulse with  $\theta_{in}$  so close to  $\pi$  that it will not change its total area in one passage through the rod. The energy (taken from Fig. 2) will change so that  $\tau_{out} \approx \tau_{in} \exp(-\frac{1}{2}\alpha L)$ . From the condition that  $\tau(z)\hat{t}(z) \approx \theta^2(z)$  and recalling that  $\theta$  remains constant, we can deduce that the output-pulse width is  $\hat{t}_{out} \approx \hat{t}_{in} \exp(\frac{1}{2}\alpha L)$ . Under conditions<sup>6</sup> where  $\hat{t}_{out} \gg \hat{t}_{in}$  it is reasonable to approximate the delay time by  $t_D \approx \frac{1}{2}\hat{t}_{out}$ . Thus we arrive at an estimate of the delay time for a  $\pi$  pulse which is  $t_D \approx (\frac{1}{2}\hat{t}_{in}) \exp(\frac{1}{2}\alpha L)$ . For our choice of parameters, this leads to an estimate of delay time which is an order of magnitude larger than the delay time for  $\theta_{in} \approx 2\pi$ . This large delay time is apparent in Fig. 3.

Thus far we have been considering the time dependence of the pulse under the "ideal" circumstances  $T_1$  and  $T_2$  much greater than  $\hat{t}$ , with no scattering losses and no detuning of the atomic system. In as much as these

<sup>6</sup> The condition that the output-pulse width be much larger than the input-pulse width implies that the absorption must be large ( $e^{-\alpha L} \ll 1$ ). For a weak attenuator the delay time for a  $\pi$  pulse is not as large as the  $2\pi$  delay. The maximum delay is for a pulse slightly less than  $2\pi$ . The delay times in the region around  $2\pi$  are discussed in Ref. 2 and in a new publication by the authors of Ref. 1.

conditions are not met in practice we now turn to a discussion of how the previous results are modified when we vary these parameters.

Since we are interested in the nonlinear effects, in all that follows we will keep the small-signal attenuation  $\tau_{out}/\tau_{in}$  the same for each case (i.e.,  $\tau_{out}/\tau_{in}$  is always 0.0012).

*Effects of atomic phase diffusion ( $T_2$ ).* Here we investigate the consequences of allowing the atomic system to have a finite memory time  $T_2$ . We note that the large delays at  $\theta_{in} \approx \pi$  are more sensitive to  $T_2$  than the delays at  $\theta_{in} \approx 2\pi$ . This is evident since the phase-memory time must be long compared to the output pulse for the effect to be seen and the output pulse is much wider than the input. The broken curves in Fig. 3 show the delay times when  $T_2$  is five and fifteen times longer than the input-pulse width. The delay for the  $\pi$  pulse is seen to vary considerably whereas the  $2\pi$  delay is changed very little. The effect of  $T_2$  on the energy behavior of the system is to raise the transition point slightly and to eliminate the transparency<sup>7</sup> at  $\theta_{in} = 2\pi$  (see Fig. 2).

*Effects of atomic lifetimes ( $T_1$ ).* In low-pressure gases it is reasonable to expect  $T_1$  and  $T_2$  to be comparable. We have, accordingly, carried out several calculations for the case  $T_2 = 150$  nsec,  $T_1 = 150$  nsec. The modifications of the theory to include  $T_1$  are found in Ref. 3. One finds, for this case, that one has a further reduction in the maximum delay time ( $t_D \approx 30$  nsec) and a slightly higher value for  $\theta_{in}$  at the transition point.

*Variation of loss per unit length ( $\kappa$ ).* The presence of a small linear loss  $\kappa$  has the effect of shifting the maximum delay to higher values of  $\theta_{in}$  and tends to produce somewhat larger maximum delays. Because it is linear and hence independent of  $\theta_{in}$ , the loss prevents any complete transparency. One notes that  $\tau_{out}/\tau_{in}$  is always less than  $e^{-2\kappa L}$ .

*Shift of the inhomogeneous line center from the carrier frequency.* The effect of having a center frequency in our medium different from the carrier frequency has received a limited amount of investigation in this work. To date, the results indicate that there is no effect produced by a small amount of detuning. This is in agreement with the results of McCall and Hahn who found one could obtain  $2\pi$  hyperbolic-secant pulses even if the system were detuned.

In conclusion, we emphasize (as was first noted by McCall and Hahn) that the self-induced transparency effect is shown most dramatically in its effect on pulse delay. In fact, Fig. 2 shows that the curves corresponding to self-induced transparency (SIT) and saturation are not dramatically different in shape, except in the region  $\tau(L)/\tau(0) \approx 1$ . These differences are not readily observable in the usual experiments. One might

<sup>7</sup> By transparency, we mean that  $\tau_{out} = \tau_{in}$  to within the limit of accuracy of the computer program (2 or 3% for the  $2\pi$  pulse). The transition point is the point on the curve of  $\tau_{out}/\tau_{in}$  versus  $\tau_{in}$  for which  $\tau_{out}/\tau_{in} = \exp(-\frac{1}{2}\alpha L)$ .

argue that the curves (for SIT and saturation) are displaced by a significant amount, however, this displacement is meaningful only if the dipole moment  $\varphi$  is known. A measurement of the amplitude of the peak of the power spectrum can be used as a direct verification of the area theorem.<sup>1</sup> The spectrum would also help to

show whether the carrier could be properly described as a monochromatic wave, or whether there were fast frequency changes present.

We wish to acknowledge helpful and stimulating conversations with Professor E. Hahn and Professor A. Szoke.

## Rotating-Frame Double Resonance and Nuclear Cross Relaxation in LiF<sup>†</sup>

DAVID V. LANG\* AND P. R. MORAN

*Department of Physics, University of Wisconsin, Madison, Wisconsin 53606*

(Received 4 March 1969; revised manuscript received 8 September 1969)

This paper reports our study of Hartmann and Hahn's technique of rotating-frame nuclear double resonance (RFDR). We consider the Li<sup>6</sup>-Li<sup>7</sup> system in LiF and obtain the cross-relaxation dynamics from the Li<sup>7</sup> free-induction-decay data via a general expression which we derive. We find that the presence of F<sup>19</sup> spins, which constitute a third species interacting strongly with the Li systems in LiF, may easily be taken into account, and that the resulting RFDR behavior does not differ qualitatively from that in a simple two-species system. The cross-relaxation time dependence is well described by an exponential or sum of exponentials for times longer than the order of  $T_2$ , with nonexponential behavior for shorter times. The cross-relaxation rate  $W_{CR}$  exhibits a Lorentzian dependence on the magnitude of the Li<sup>6</sup> rf field,  $H_{16}$ , for the case where the Li<sup>7</sup> system has been adiabatically demagnetized in the rotating frame; these results show that the Gaussian behavior previously assumed is incorrect. For the case where the Li<sup>7</sup> rf field is of the order of the local field,  $W_{CR}(H_{16})$  is asymmetric about Hahn's double resonance (DR) condition, with the larger  $W_{CR}$  corresponding to  $H_{16}$  less than for the DR condition. The cross-relaxation times at the DR condition are on the order of 0.4 msec. We observe no spin-diffusion bottleneck in a sample of LiF with an isotopic abundance of 0.008% Li<sup>6</sup>. Finally, we draw some general conclusions about the application of RFDR to other problems.

### I. INTRODUCTION

NUCLEAR double resonance in the rotating frame (RFDR) was first suggested as an ultrahigh-sensitivity NMR technique in 1960 by Hartmann and Hahn.<sup>1</sup> The classic analyses of the method have been given by Hartmann and Hahn<sup>2</sup> (hereafter referred to as HH) using the general density matrix techniques, and by Lurie and Slichter<sup>3</sup> (hereafter referred to as LS) using a thermodynamic treatment. Several groups have used variations of this technique to obtain NMR and NQR spectra of rare isotopes or impurities in solids.<sup>3-14</sup>

The work reported here is primarily an experimental study of the RFDR method itself rather than an application of the method to obtain high-sensitivity spectra of a particular solid.

The reader is referred to the excellent descriptions of the general technique given in HH and LS. In Sec. II, we will review these basic ideas principally as a means of introducing our notation.

We consider two nuclear-spin systems with strong resonant rf fields applied to each. The proper way to describe such a system is in a double rotating-frame representation.<sup>2,3</sup> In this representation, each of the two spin species can be made to sense a different "effective field," and thus the effective Zeeman splittings of the two species can be made equal, thereby allowing rapid cross relaxation. This condition of equal effective field splittings is called the double resonance (DR) or Hahn condition.

The standard method of high-sensitivity spectroscopy is then as follows. The rare-species resonance system is modulated in such a way as to pump energy into the rare-spin effective Zeeman levels. This pumped energy

<sup>†</sup> Work supported under Grant Nos. AFOSR-1065-66 and 69-1749 of the U. S. Air Force Office of Scientific Research.

\* N. S. F. Predoctoral Fellow; present address: Department of Physics, University of Illinois, Urbana, Ill.

<sup>1</sup> S. R. Hartmann and E. L. Hahn, *Bull. Am. Phys. Soc.* **5**, 498 (1960).

<sup>2</sup> S. R. Hartmann and E. L. Hahn, *Phys. Rev.* **128**, 2042 (1962).

<sup>3</sup> F. M. Lurie and C. P. Slichter, *Phys. Rev.* **133**, A1108 (1964).

<sup>4</sup> A. G. Redfield, *Phys. Rev.* **130**, 589 (1963).

<sup>5</sup> R. E. Walstedt, D. A. McArthur, and E. L. Hahn, *Phys. Letters* **15**, 7 (1965).

<sup>6</sup> Y. Tsutsumi, M. Kunitomo, and T. Hashi, *J. Phys. Soc. Japan* **20**, 2095 (1965).

<sup>7</sup> R. E. Slusher and E. L. Hahn, *Phys. Rev. Letters* **12**, 246 (1964).

<sup>8</sup> A. Hartland, *Phys. Letters* **20**, 567 (1966).

<sup>9</sup> M. Satoh, P. R. Spencer, and C. P. Slichter, *J. Phys. Soc. Japan* **22**, 666 (1967).

<sup>10</sup> G. T. Mallick and R. T. Schumacher, *Phys. Rev.* **166**, 350 (1968).

<sup>11</sup> A. Hartland, *Proc. Roy. Soc. (London)* **A304**, 361 (1968).

<sup>12</sup> R. E. Slusher and E. L. Hahn, *Phys. Rev.* **166**, 332 (1968).

<sup>13</sup> K. F. Nelson and W. D. Ohlsen, *Phys. Rev.* **180**, 366 (1969).

<sup>14</sup> E. L. Hahn, *Nuclear Magnetic Resonance and Relaxation in Solids* (North-Holland Publishing Co., Amsterdam, 1965), p. 42.